

## EXPERIMENTAL INVESTIGATION OF FLOW CHARACTERISTICS INSIDE AN AXISYMMETRIC CAVITY OF A SHROUDED SINGLE-STAGE COMPRESSOR USING A FIVE-HOLE PROBE

V. G. Gkoutzamanis, T. G. Efstathiadis, S. N. Theodorou, A. I. Kalfas

Laboratory of Fluid Mechanics and Turbomachinery  
Department of Mechanical Engineering  
Aristotle University of Thessaloniki,  
Greece

**Keywords:** axisymmetric cavity, shrouded single-stage compressor, five-hole probe

### ABSTRACT

The present work constitutes an experimental study of the three-dimensional flow field inside the axisymmetric cavity of a shrouded single-stage compressor.

The experimental setup contains an open, low speed wind tunnel, an axisymmetric cavity with a profile of sudden enlargement at the inlet and sudden contraction at the outlet and the compressor stage. The measurements are conducted with a 5-hole Cobra-shaped probe, as its miniscule dimensions make it suitable for highly three-dimensional flow phenomena. The measurement procedure consists of three different cases. In the first case the blades are stationary and the measurements are conducted in a plane perpendicular to the main flow direction ( $r-\theta$  plane). The second case contains the measurements taken in a plane parallel to the main flow and perpendicular to the compressor ( $r-x$  plane). The third case represents the rotating stage experiment, where measurements are taken downstream the stage.

Results show that a three-dimensional flow between the opposite sides of the blades is spotted where part of the fluid moves from the pressure side to the cavity and another part moves from the cavity to the suction side. Furthermore, a structure of vortices is found downward the shroud in the form of a counter-rotating vorticity dipole. The dipole moves downward to the cavity affecting both the toroidal vortex of the corner and the main flow exiting the compression stage.

### NOMENCLATURE

#### *Symbols*

H	Cavity height [mm]
L	Cavity length [mm]
PS	Pressure Side [-]
R	Radius [mm]
SS	Suction Side [-]
$V_\infty$	Freestream velocity [m/s]
$\nu$	Kinematic Viscosity [m <sup>2</sup> /s]

### INTRODUCTION

In recent years, progress in aviation industry has brought about the demand for the improvement of the various turbomachinery mechanisms that incur losses to the aircraft engines, thus decreasing their efficiency. In particular, one such mechanism are the cavities that reside in all of the gas turbine components (compressor, combustor, turbine). A cavity subcategory is the axisymmetric cavity which has recently drawn significant attention, due to the complexity of the flow phenomena that occur in these geometrical features. Cavities have an effect on the flow field, thus generating loss mechanisms through pressure fluctuations and the vortex shedding effect. As far as compressors are concerned, axisymmetric cavities of specific profile can be found, namely the swan neck ducts, leading to secondary flows and incurring significant losses.

According to the research available in the literature, the published work for axisymmetric cavities of shrouded compressors is limited. Ezhil Kumar & Mishra (2012) studied numerically the effects of secondary air jet momentum on cavity flow structure, under reacting and non-reacting flow conditions.

Rusch et al. (2004), introduced a novel technique of analytical study of complex flow fields involving vortical structures in axisymmetric cavity flows.

Yao et al. (2001) investigated numerically the effect of unsteady incompressible flow over three dimensional cavities. Faure et al. (2007) performed visualization studies in order to understand the spatial development of dynamical structures inside an open cavity, at medium range Reynolds numbers.

Lee and Sung (1994) performed an experimental study of turbulent axisymmetric cavity flow for three values of cavity length and a fixed value of cavity height. The flow configuration consists of a sudden expansion and contraction pipe joint, which is approximately close to the geometry studied herein.

Having discussed the above, the aim of this work is the experimental investigation of the flow characteristics created at the inlet and outlet of the cavity as well as its impact on the main flow that passes through the blades.

### AXISYMMETRIC CAVITIES

A key issue for designing better turbomachinery components is to understand the flow interactions set up by the presence of labyrinth seals. It is important to quantify the secondary flow development and mixing losses (Pfau et al. 2004). Significantly high adverse pressure and velocity gradients can be found in cavities that exist in all of the engines components.

The axisymmetric cavity that is studied here is characterized by a profile of a sudden enlargement at the inlet and sudden contraction at the outlet. In general, cavities can be classified into two categories. The first one (Figure 1) considers geometrical features. More specifically, the ratio of the length ( $L$ ) over the step height ( $H$ ). On the other hand, the second classification (Tracy & Plentovich, 1997) of cavities considers the flow field type.

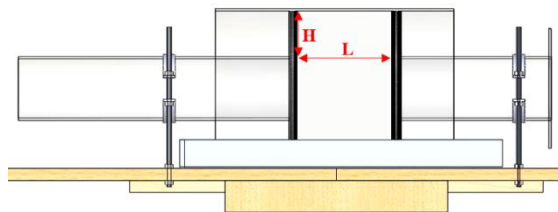


Figure 1: Representation of the geometrical features of a cavity

There can be three types of cavities according to the flow field type:

- First, for sufficiently large  $L/H$  ratios (values of greater than or equal to 13), separation of the flow can be observed at the inlet, followed by reattachment at a point which depends on the absolute length of the cavity and the dynamic characteristics of the flow field and finally, a second separation before the contraction of the outlet. This is termed a closed cavity.
- Second, for small  $L/H$  ratios (values of less than or equal to 10). It is observed that the separated flow does not reattach to the wall and the cavity of inlet and outlet are bridged by the shear layer formed over the cavity. In this case, a recirculation zone covers the entire cavity length. This is termed an open cavity.
- Third type of cavity flows includes the transitional cavities for intermediate  $L/H$  ratios.

The occurrence of the abovementioned flow field types also depends on the free-stream Mach number and hence, whether the flow is characterized by a supersonic speed or not. This

will not be further analyzed as the current investigation considers subsonic flow behavior.

### EXPERIMENTAL METHODS

#### Test rig

The experimental setup, as shown in Figure 2, is an open, low speed wind tunnel, which serves as a mass flow generator, an axisymmetric cavity with a profile of sudden enlargement at the inlet and sudden contraction at the outlet and the compressor stage.

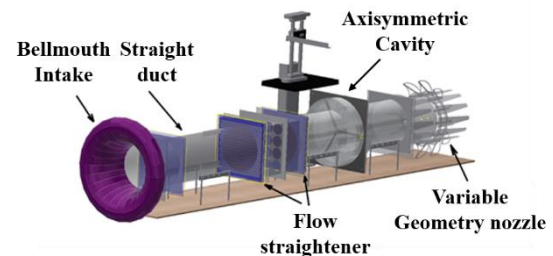


Figure 2: 3D representation of the experimental setup used for the investigation of the flow field inside the axisymmetric cavity

The wind tunnel is designed and built at the Laboratory of Fluid Mechanics and Turbomachinery (LFMT) of Aristotle University of Thessaloniki (AUTH) (Vouros et al., 2016). For the purposes of this study, it has been adjusted to include the part of the axisymmetric cavity. Its design and manufacturing is the result of this study. Moreover, the other various parts of the wind tunnel are a bellmouth intake nozzle, the flow conditioning elements, a variable geometry exit nozzle and the fan stacks that generate mass flow. The mass flow can be controlled by either changing the power supply of the fans or the position of the exit nozzle.

Considering the fan stacks which are required for the production of the required mass flow, these are small axial fans used for the cooling of the CPU units. They can be either placed in series or in parallel, with the most fundamental prerequisite being to maintain their symmetry with regard to the wind tunnel axis. The fan stacks simulate the compressor unit and consist of 16 fans placed in parallel. The performance evaluation of this type of fan has been studied numerous times in the aforementioned laboratory and more details can be found in the literature (Terzis et al., 2009).

Regarding the axisymmetric cavity, it is created in order to study the flow field in a compressor channel. Hence, an enclosed fan is placed (Figure 3a) in order to represent a rotor blade row. The type of fan is similar to a vehicle cooling fan. Its goal is to simulate the flow field both in the cavity and along the blades downstream of the flow. In terms of design characteristics, this setup is close to steam turbine cavities, having larger tip clearances upstream and downstream the

compressor stage. The axisymmetric cavity setup is manufactured by acrylic glass to facilitate for the visualization of the flow. As already discussed previously, the two parameters that define the flow behavior are the length (L) and step height (H) of the cavity.

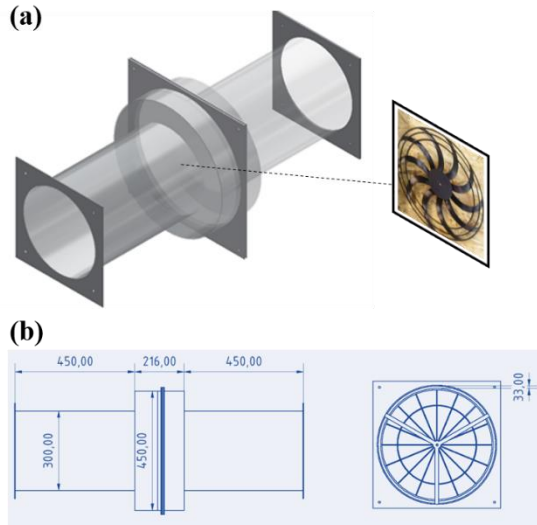


Figure 3: (a) Setup for the study of axisymmetric cavity together with the enclosed blade row, (b) design plan of the axisymmetric cavity

As it can be also observed in Figure 3b, the geometrical characteristics of the cavity are the following:

- Length over height ratio:  $L/H = 2.88 [-]$
- Tip clearance length:  $y = 33 [mm]$

The tip clearance length is defined as the distance between the wall and the shroud of the compressor stage.

### Measurement techniques

There are complex phenomena (three-dimensional) which unfold in such geometrical features of sudden enlargements or contractions. Hence, in order to analyze them, both magnitude and direction must be defined to measure velocity components. For this reason, detailed pressure measurements are necessary and miniature pressure probes can facilitate accurate measurements.

For the purposes of this study, pressure measurements inside the flow-field are conducted with a pneumatic 5-hole Cobra-shaped probe.

Using this type of probe provides an exact known measuring location, given that probe's tip is located exactly at the extension of the stem's longitudinal axis. In addition, "Cobra" shape minimizes the flow blockage effect on the local measuring location as the probe's stem is faraway and allows the probe to approach the walls, where boundary layer interactions take place and are of great importance in turbomachinery (Magkoutas et al., 2016).

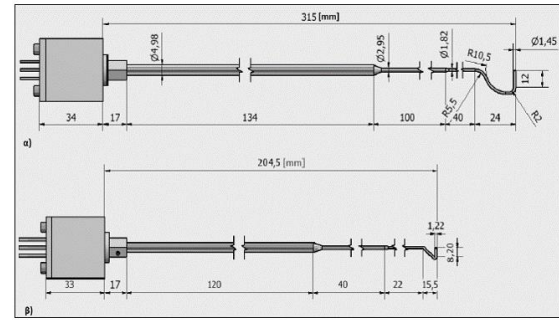


Figure 4: The two Cobra-shaped five-hole probes fabricated and calibrated in LFMT, used for the purposes of this study

The design and fabrication of five-hole pressure probe, in small dimensions, constitute considerably difficult and delicate tasks that require significant expertise. The Cobra-shaped probe is manufactured by stainless steel, with a tip diameter as small as 1.45mm, ensuring a minimally invasive and highly accurate method for the investigation of the flow.

Two probes are manufactured and calibrated in LFMT, demonstrating good overall behavior concerning its accuracy. The two probes differ in their total length.

All pressure measurements are combined with a pneumatic pressure scanner (Netscanner 9116) and an engineering software for data acquisition. The full-scale measurement accuracy of the pressure scanner is 0.05%. The non-nulling calibration method is employed for the Cobra-shaped probe (Lee & Jun, 2003) as it is widely used and well known. Processing of the pressure data is based on the Treaster and Yocum (1978) algorithm. The calibration range is considered reliable within a  $\pm 30^\circ$  range for both angular planes. Reduced uncertainty of measurements can be achieved if the probe is used within a  $\pm 20^\circ$  range, which is highly suggested.

### RESULTS ANALYSIS

The measurement procedure consists of three different cases, the results of which are presented in a separate section. Therefore, in the first case, the blades are stationary and the measurements are conducted in a plane perpendicular to the main flow direction ( $r-\theta$  plane). Aim of that set of measurements is to extract the pressure and velocity fields along the compressor stage as well as inside the cavity. The second case contains the measurements taken in a plane parallel to the main flow and perpendicular to the compressor ( $r-x$  plane). Supplementary measurements are taken in this case to create the flow's vorticity fields. The third case represents the rotating stage experiment. Measurements are taken downstream the stage. This leads to the extraction of pressure and velocity profiles along the radius of the stage and inside the cavity.

### Stationary stage experiment

In the first case, the goal is to extract the pressure and velocity field downstream the compressor stage. For this reason, the variable nozzle geometry has been placed in such a way, so that it constitutes a straight duct and the fan array providing the maximum available power, in order to overcome the fluid flow distortion induced by the geometrical shape of the sudden enlargement and contraction of the cavity area. Therefore, the freestream velocity is measured at  $U_\infty = 6.8$  m/s. Taking into consideration the conditions under which the current measurements take place, the Reynolds number having the wind tunnel diameter as a characteristic length is calculated to be equals to:

$$Re_d = \frac{U_\infty * d_{tunnel}}{\nu} = 1.3 * 10^5$$

On the other hand, taking the diameter of the cavity as the characteristic length, the Reynolds number is calculated as follows:

$$Re_{d,cav} = \frac{U_\infty * d_{cavity}}{\nu} = 1.95 * 10^5$$

Regarding the geometrical characteristics of the first case of measurements, the probe is placed at the upper side through a small aperture, in the middle of the downstream part of the cavity ( $x/L=0.75$ ), as shown in Figure 5.

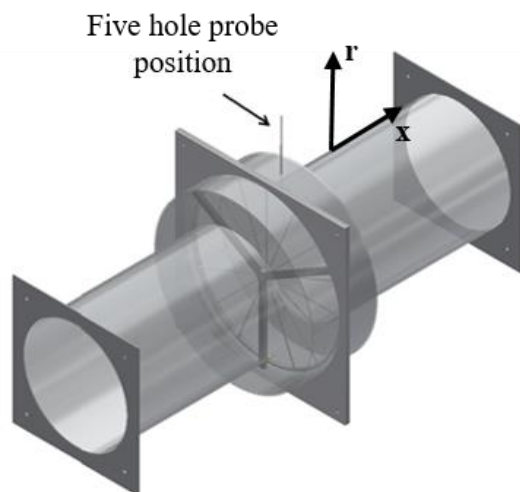


Figure 5: First case measurements

The measurement grid (Figure 6) consists of 620 points (31x20) in r-θ plane and the region of the channel on both sides of the blade.

The conduction of measurements and data processing as it has been described in section 'Measurement Techniques' is based on the non-nulling mode.

The results of this case show areas of high pressures inside the channels and low pressures along the blade, as expected and shown in the isolines of total pressure (Figure 7).

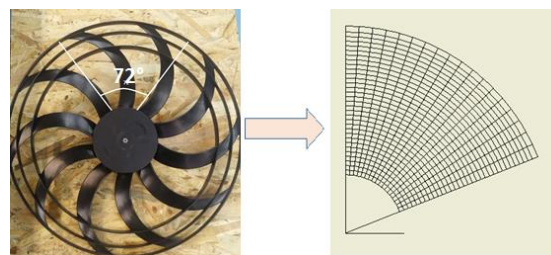


Figure 6: Measurement grid

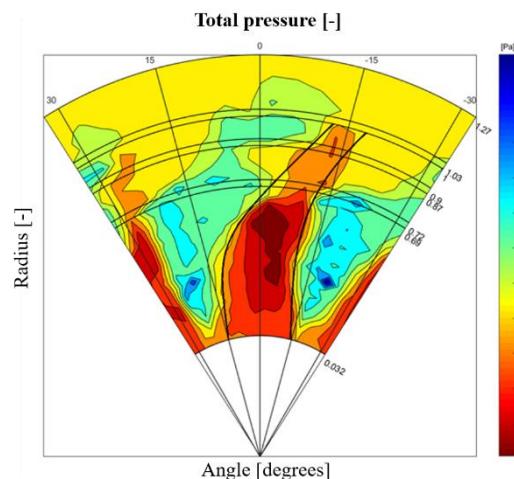


Figure 7: Iso-lines of total pressure. The black line indicates the position of the blade

Additionally, the effect of the shrouded stage can be observed, because of the non-continuous fluctuations of pressure inside and outside of the blade tip areas. Moreover, a diffusion of the flow crossing the compressor stage towards the area of the cavity and which is characterized by constant pressure can be observed.

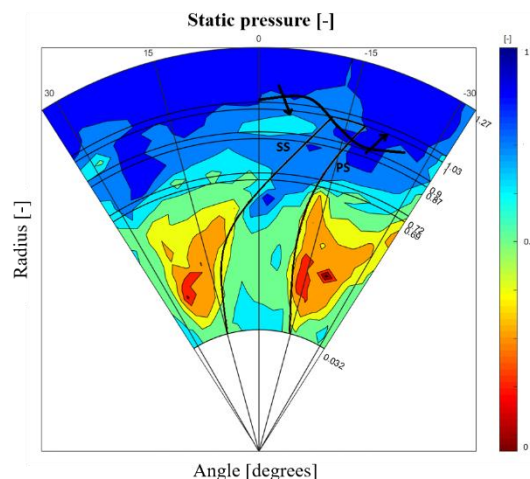


Figure 8: Iso-lines of static pressure

Continuing with the analysis of the first case results, Figure 8 provides more information. The area of the tip of the blade shows an area of low static pressure at the suction side (SS) of the blade and an area of higher static pressure at the pressure side (PS). This leads to the conclusion that there is

an inflow from the cavity to the blade channel, on the suction side. On the other hand, an outflow can be seen on the pressure side, with a direction from the blade channel to the cavity side. This observation verifies the highly three-dimensional flow as it also has an effect on the bypass flow and the evolution of flow inside the cavity.

### Measurements inside cavity

Regarding the geometrical characteristics of the second case, measurements are conducted in a plane parallel to the main flow and perpendicular to the compressor (r-x plane). The probe is placed downstream the shrouded compressor stage ( $x/L=0.505$ ) as also shown in Figure 9.

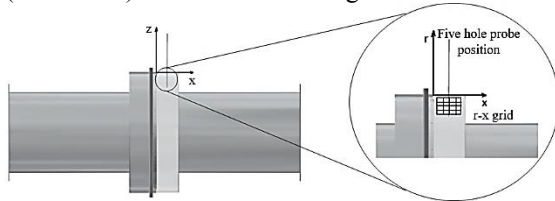


Figure 9: Second case measurements

The measurements of the probe are conducted by plunging the probe at the r-direction with a step of 5 mm and a range of 25 mm. Similarly, the axial displacement is done with a 5-mm step and a range of 25 mm. Measurements are conducted in nulling mode (yaw angle). The probe is rotated in 12 different angular positions. The grid consists of 300 points in the r-x plane.

The results of this part of measurements show an area of low static pressure downstream the shroud. Additionally, the area of high static pressure is close to the cavity corner. This area is associated to the local narrowing that occurs due to the interference of the shroud to the flow direction and to the immediate enlargement after that point. The area of low pressure is mainly affected by the main flow that is characterized by higher kinetic energy than the flow in the cavity. A general conclusion that is drawn is the intense tendency of the flow to turn towards the area where main flow dominates.

Another conclusion can be drawn from Figure 11. It can be observed that the flow is characterized by high swirl, due to increased flow angles as compared to the respective angles of the main flow. Its maximum value is observed over the shroud. Therefore, an upstream 'turning' of the flow is also applied from the blades of the compressor stage due to the lower inertia that characterizes the flow inside the cavity. This behavior combined with the results from the measurements upstream the stage give rise to a Couette flow between the shroud and the wall of the cavity. That is the flow of a fluid in the space between two surfaces. This behavior is verified in the following paragraphs.

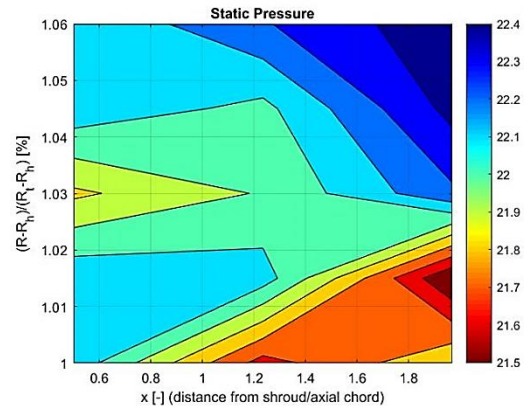


Figure 10: Iso-lines of static pressure downstream the axisymmetric cavity

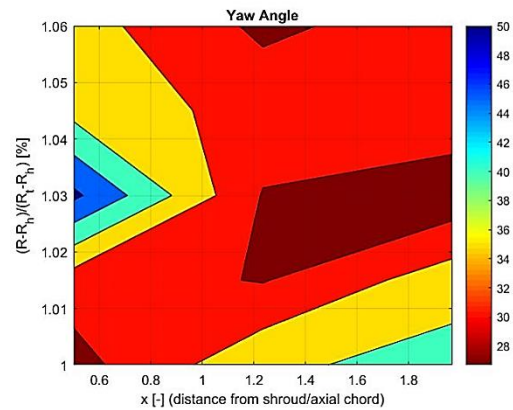


Figure 11: Iso-lines of yaw angle downstream the axisymmetric cavity

In order to perform more thorough analysis regarding the flow inside the cavity, some additional measurements were taken, utilizing a dense grid in particular positions of the previous part of this case. This time, the measuring step was altered to 0.5 mm for the displacement in the r and x directions.

The diagram of the vorticity iso-lines verifies the abovementioned indication of Couette flow characteristics which indicates a structure of vortices downward the shroud in the form of a counter-rotating vorticity dipole (Figure 12).

The initialization of this structure can be observed in area A of the figure above. Its propagation to area B is followed by an enlargement of this structure which verifies the existence of the vorticity dipole. The main flow adds kinetic energy to the negative pole and the bypass flow adds energy to the positive flow, thus forming the two counter-rotating vortices.

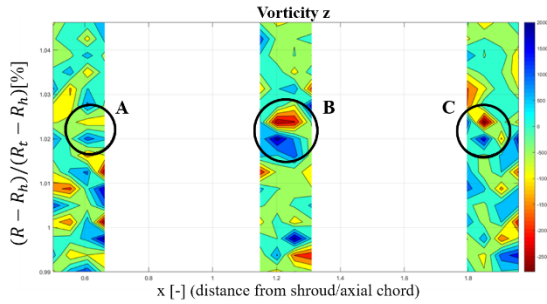


Figure 12: Iso-lines of tangential vorticity

The tangential vorticity distribution (Figure 13) verifies the occurrence of a dipole of counter-rotating vortices right after the shrouded blades. Positive values of vorticity indicate right-handed rotation while negative values correspond to left-handed rotation. The dipole is formed by the shear layer of the upper and lower flow field downstream the shroud. It is also observed that the negative pole diminishes faster as compared to the positive pole and that is associated to the main flow effect and the descending direction of the bypass flow. The occurrence of intense shear on the flow as it escapes the shroud, is the cause of these instabilities.

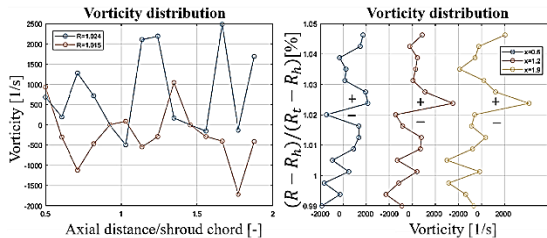


Figure 13: Tangential vorticity distribution

Last but not least, Figure 14 demonstrates that vorticity tends to decay. The average increase of the negative values of vorticity is associated to the energy it takes from the main flow.

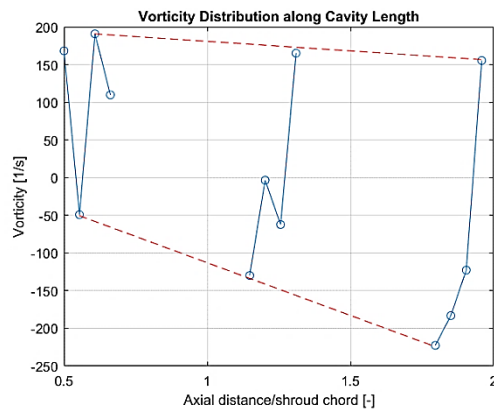


Figure 14: Vorticity distribution along cavity length

### Rotating stage experiment

The third case considers measurements downstream the blades for a rotating stage

experiment. The probe is plunged vertically ( $x/L=0.75$ ) in two points ( $0^\circ$  and  $15^\circ$ ) due to the expected stratification of the flow field.

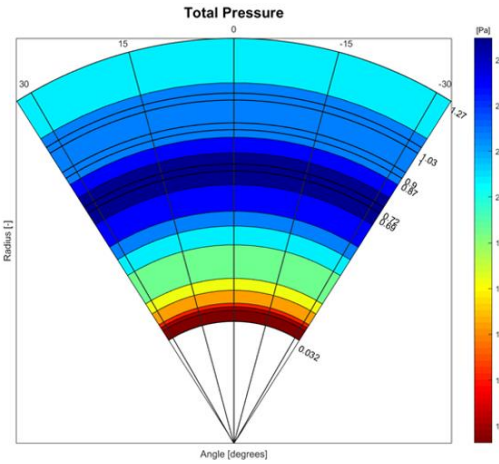


Figure 15: Iso-lines of total pressure for the rotating stage

The plunging step is 1 mm and the grid consists of 320 points ( $160 \times 2$ ). Measurements revealed the existence of the expected stratified flow (Figure 15).

The higher-pressure area is found near the first (inner) shroud. A pressure drop is then observed until the position of the outer shroud, followed by a nearly constant pressure distribution inside the cavity area. The lower pressure area at the hub of the blades is caused by a local disruption of the flow-field as no guiding component exists to drive the flow towards the blades where measurements are conducted.

The abovementioned conclusions can be better demonstrated in the following total pressure and velocity diagrams.

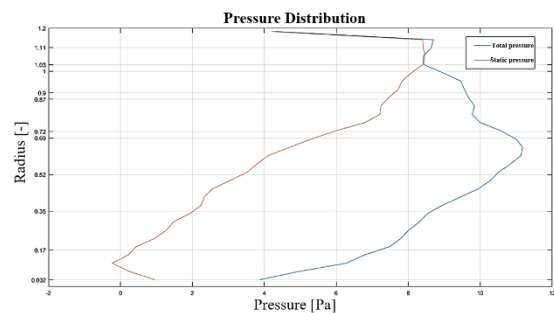


Figure 16: Mass-averaged total and static pressure distribution

The mass-averaged total pressure distribution diagram (Figure 16) indicates an adverse static pressure gradient at the rotor's hub which is caused by the local convergence of the streamlines that fall onto the hindrance of the rotor's disk. The flow is locally accelerated at this point. According to the velocity diagram (Figure 17), a flow 'jump' is observed for the  $w$  component ( $z$ -direction) which

is linked to the pitch angle and more specifically the flow rise due to the existence of the hindrance.

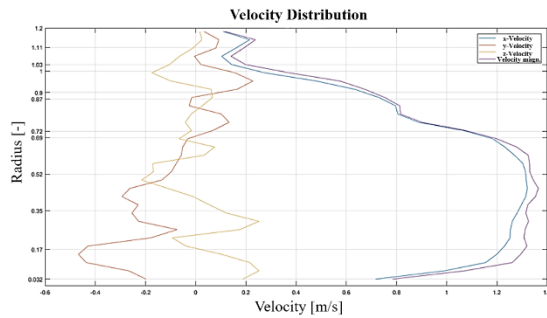


Figure 17: Mass-averaged velocity distribution

After the hub point and until the  $R=1.03$  point, which is the end point of the shroud, the static pressure is monotonically increasing. The static pressure inside the cavity remains constant until the point  $R=1.16$  where an adverse pressure gradient is revealed, due to the walls' effect.

As regards with the total pressure, it is increasing due to the work addition from the compressor's rotation to the fluid.

Velocity distribution diagram indicates that components  $v$ ,  $w$  (for the directions  $y$  and  $z$  respectively) are almost zero with infinitesimal deviation. Additionally, the velocity profile from the hub of the blade until the first shroud-ring is parabolic, with local maximum at point  $r=0.41$ . After that point, a large decrease is observed until the end of the third shroud-ring. At the cavity area, a small velocity increase is measured due to the kinetic energy that is added to the flow from the rotation of the stage. The flow at the upper part of the outer ring is close to a Couette flow and for this reason, the swirl measured in this area is intense, as already described previously.

## CONCLUSIONS

The current work performs an experimental study of a configuration that simulates the three-dimensional flow field inside the axisymmetric cavities of a shrouded single-stage compressor. Two miniscule 'Cobra' shaped five-hole probes have been used in an open circuit wind tunnel, adjusted in order to simulate the flow-field of an axisymmetric cavity. Of the three different cases that are examined (stationary stage experiment, rotating stage experiment and measurements inside the cavity) the most important findings can be summarized as follows:

- The calibration range is considered reliable within a  $\pm 30\%$  measurement range for both angular planes (yaw and pitch direction). Reduced uncertainty of measurements can be achieved if the probe is used within a  $\pm 20\%$  range, which is highly suggested.
- The flow 'jump' that rises from the pressure side to the cavity side and from the cavity side

to the suction side has an overall effect to the channel flow and incurs three-dimensional disturbances.

- The rotating stage gives rise to Couette flow condition at the upper part of the outer shroud thus leading to extreme yaw angles.
- The tangential vorticity distribution verifies the occurrence of a dipole of counter-rotating vortices moving downstream the flow until the sudden wall contraction point of the cavity. As a result, both the toroidal vortex of the corner and the main flow exiting the compression stage are affected.
- The bypass flow at the point downstream the shroud moves intensely downwards, affecting the inlet velocity field for the stationary stage of the blades that follows in a real gas-turbine setup. Part of this flow also contributes to the regeneration of the toroidal vortex.
- The bypass flow at the point upstream the shroud moves intensely upwards, diminishing the velocity field that is introduced at the compressor's rotor.

## REFERENCES

- [1] Ezhil Kumar, P. K.; Mishra D. P.; 2012. "Numerical simulation of cavity flow structure in an axisymmetric trapped vortex combustor". *Aerospace Science and Technology*, vol. 21 (2012), pp. 16-23.
- [2] Rusch, D.; Pfau, A.; Schlienger, J.; Kalfas, A. I.; Abhari, R. S.; 2003. "Deterministic Unsteady Vorticity Field in a Driven Axisymmetric Cavity Flow". *Journal of Computational and Applied Mechanics*, vol. 5 (2), pp. 353-365.
- [3] Yao, H.; Cooper, R. K. & Raghunathan, S.; 2004. "Numerical Simulations of Incompressible Laminar Flow over Three-Dimensional Cavities". *Journal of Fluids Engineering*, vol. 126, pp. 919-927.
- [4] Faure, T. M.; Adrianos, P.; Lusseyran, F. & Pastur, L.; 2007. "Visualizations of the flow inside an open cavity at medium range Reynolds numbers". *Experiments in Fluids*, 42(2), pp. 169-184.
- [5] Lee, D. H. & Sung H. J.; 1994. "Experimental Study of Turbulent Axisymmetric Cavity Flow". *Experiments in Fluids*. Vol. 17, pp. 272-281.
- [6] Tracy, M. B. & Plentovich, E. B.; 1997. "Cavity Unsteady-Pressure Measurements at Subsonic and Transonic Speeds". NASA Technical Paper 3669, National Aeronautics and Space Administration, Langley Research Center, Virginia 23681-2199.

- [7] Vouros, S. V.; Chasoglou, A. C.; Efstathiadis T. G.; Kalfas, A. I.; 2016. "Effects of Rotor-Speed-Ratio and Crosswind inlet distortion on Off-Design Performance of Contra-Rotating Propelling". Proceedings of ASME Turbo Expo 2016: Turbomachinery Technical Conference and Exposition, June 13-17, Seoul, South Korea. GT2016-57273.
- [8] Terzis, A.; Kyprianidis, K.; Zachos, P.; Kalfas A. I.; 2009. "Comparative Performance Evaluation of a Multistage Axial Fan Assembly". XIX International Symposium on Air Breathing Engines (ISABE), (ISABE-2009-1187).
- [9] Magkoutas, K. I.; Efstathiadis, G. T.; Kalfas, A. I.; 2016. "Experimental Investigation of Geometry Effects and Performance of Five-Hole Probe in Measuring Jets in Crossflow". The 23<sup>rd</sup> Symposium on Measuring Techniques in Transonic and Supersonic Flows in Cascades and Turbomachines, Stuttgart, Germany.
- [10] Dominy, R. G. & Hodson, H. P.; 1993. "An investigation of Factors Influencing the Calibration of 5-Hole Probes for 3-D Flow Measurements". Journal of Turbomachinery, 115(3), pp. 513-519.
- [11] Lee, S. W. & Jun, S. B.; 2003. "Effects of Reynolds Number on the Non-Nulling Calibration of a Cone-Type Five-Hole Probe". Proceedings of ASME Turbo Expo: Power for Land, Sea & Air, Atlanta, Georgia, USA, June 16-19, 2003 (GT2003-38147).
- [12] Treaster A. L.; Yocum A.; 1978. "The calibration and application of five-hole probes". ISA Transactions 18 (3)
- [13] Pfau, A.; Kalfas, A. I. & Abhari, R. S.; 2007. "Making Use of Labyrinth Interaction Flow". Journal of Turbomachinery, vol. 129, pp. 164-174.
- [14] Pfau, A.; Schlienger, J.; Kalfas, A. I. & Abhari, R. S.; 2002. "Virtual Four Sensor Fast Response Aerodynamic Probe (FRAP)". Cambridge, The 16<sup>th</sup> Symposium on Measuring Techniques in Transonic and Supersonic Flows in Cascades and Turbomachines.
- [15] Schlienger, J.; Pfau, A.; Kalfas, A. I. & Abhari, R. S.; 2003. "Measuring Unsteady 3D Flow with a Single Pressure Transducer". European Turbomachinery Conference.
- [16] Telionis, D.; Yang, Y. & Rediniotis, O.; 2009. "Recent developments in Multi-Hole Probe Technology". Proceedings of COBEM 2009, 20<sup>th</sup> International Congress of Mechanical Engineering, Gramado, COBEM.
- [17] Argüelles Diaz, K. M.; Fernández Oro, J. M.; Blanco Marigorta, E.; Barrio Perrotti, R.; 2010. "Head Geometry Effects on Pneumatic Three-Hole Pressure Probes for Wide Angular Range". Flow Measurement and Instrumentation, vol. 21 (2010), pp. 330-339.
- [18] Pisasale, A. J. & Ahmed, N. A.; 2002. "A Novel Method for Extending the Calibration Range of Five-Hole Probe for Highly Three-dimensional Flows". Flow Measurement and Instrumentation, pp. 23-30.
- [19] Georgiou, D. P. & Milidonis K. F.; 2014. "Fabrication and Calibration of a Sub-miniature 5-hole Probe with Embedded Pressure Sensors for Use in Extremely Confined and Complex Flow Areas in Turbomachinery Research Facilities". Flow Measurement and Instrumentation, vol. 39 (2014), pp. 54-63.
- [20] Mansour, M.; Chokani, N.; Kalfas A. I.; Abhari R. S.; 2008. "Time-resolved entropy measurements using a fast response entropy probe". Measurement Science and Technology, vol. 19(11), 115401.
- [21] Town, J. & Camci, C.; 2011. "Sub-Miniature Five-Hole Probe Calibration Using a Time Efficient Pitch and Yaw Mechanism and Accuracy Improvements". Proceedings of ASME Turbo Expo Turbine Technical Conference, IGTI 2011, Vancouver, Canada, June 6-10, GT2011-46391.